Acta Scientiarum

http://periodicos.uem.br/ojs/acta
ISSN on-line: 1807-8621
Doi: 10.4025/actasciagron.v42i1.43518




# Soil water content and net precipitation spatial variability in an Atlantic forest remnant

**André Ferreira Rodrigues*, Carlos Rogério de Mello, Marcela de Castro Nunes Santos Terra, Vinicius Oliveira Silva, Gustavo Alves Pereira and Renato Antônio da Silva**

Departamento de Engenharia, Setor de Água e Solo, Universidade Federal de Lavras, Câmpus Universitário, s/n., 37200-000, Cx. Postal 3037, Lavras, Minas Gerais, Brazil. *Author for correspondence. E-mail: afrodrigues09@gmail.com

**ABSTRACT.** This study was carried out in an Atlantic forest remnant in Southeastern Brazil and aimed to spatially model the soil water content (SWC) and net precipitation (NP) on a monthly time scale and to assess the spatial behavior of these hydrological variables in the different seasons. NP is defined by summing throughfall and stemflow, which have been collected after each rain event and accumulated monthly. Soil moisture measurements were carried out monthly up to a depth of 1.00 m and then integrated to obtain the SWC. The exponential semivariogram model was fitted for both hydrological variables, and the goodness-of-fit was assessed by a cross-validation procedure, spatial dependence degree (SDD) and spatial dependence index (SDI). This model provided adequate performance for SWC and NP mapping according to the cross-validation statistics. Based on the SDD, both variables have been classified as a 'strong spatial dependence structure'. Nevertheless, when the SDI was assessed, NP showed less spatial dependence, while the SWC maintained almost the same performance. Kriging maps pictured the regional climate seasonality due to higher values of both variables in spring and summer than in autumn and winter seasons. However, correlations between NP and SWC are not expressive in the studied period.

**Keywords:** geostatistics; latosol-semideciduous forest site; forest hydrology.

Received on July 13, 2018.
Accepted on September 26, 2018

## Introduction

The hydrological cycle is the set of stages and processes that water is subject to in nature, encompassing different forms of precipitation, infiltration, recharge of aquifers, generation of surface runoff and evapotranspiration. Among these factors, the response of each phase of the water cycle is closely related to the different land use, especially in forest ecosystems (Sari, Paiva, & Paiva, 2016). Due to the natural complexity of the hydrological cycle, it is necessary to deepen the knowledge of interactions between its phases, mainly the terrestrial phase.

Soil water is one of the most important stages of the hydrological cycle. Its spatial and temporal distributions are fundamental for understanding hydrological processes, such as the generation of direct surface runoff, recharge of aquifers (percolation), evapotranspiration and soil erosion processes (Yang, Chen, Wei, Yu, & Zhang, 2014). With respect to native forests, soil moisture and its fluctuations throughout time are capable of promoting significant changes in the structure and dynamics of forests. Vale et al. (2013) observed an increase in basal area due to the rapid growth of many trees in three dry forests in the Araguari River Basin, Brazil, after increasing soil moisture due to the construction of two dams in the surrounding area.

Forest ecosystems have a direct relationship with the hydrological cycle, having a special effect on the redistribution of gross precipitation and the increase of water infiltration capability (Xu et al., 2012; Terra et al., 2018). The rainfall interception takes place when the rainfall reaches the forest canopy. A portion is retained and then evaporated to the atmosphere, a portion flows through the trunks (stemflow) and another portion passes freely by the canopy into the ground (throughfall) (Ávila, Mello, Pinto, & Silva, 2014; Bialkowski & Buttle, 2015). The set formed by the throughfall and the stemflow is known as net precipitation. In this sense, several studies have focused on the measurement and modeling of rainfall interception in forest environments (Sato, Avelar, & Netto, 2011; Ávila et al., 2014; Sari et al., 2016; Junqueira Junior et al., 2019). However, there are a lack of studies that address the variations in the hydrological cycle elements in different forest stands and analyze the idiosyncrasies of each case.

Nevertheless, these hydrological components should not be treated as local information, which may lead to errors with different degrees of relevance, since such quantities tend to have high spatial variability (Ávila, Mello, Mello, & Silva, 2011; Zucco, Brocca, Moramarco, & Morbidelli, 2014). Therefore, it is important to use procedures that seek to describe their spatial behavior, especially for soil water content (Liang, Hung, Chan, & Lu, 2014) and net precipitation, both of which have been rarely studied in tropical forests.

The application of geostatistics to spatially model net precipitation and soil water content is an important contribution for the acquisition of robust information for a better hydrological understanding of forest environments in tropical regions. Such information may imply a better prediction of forest behavior in climatic and/or land use change scenarios and culminate in better management and conservation strategies. This is particularly relevant for the Brazilian Atlantic forest, a diversity hotspot (Gorenflo, Romaine, Mittermeier, & Walker-Painemilla, 2012) that is increasingly threatened and requires special attention.

Therefore, the objectives of this study were (i) to apply geostatistical tools to study the spatial distribution of soil water content (SWC) and net precipitation (NP) in an Atlantic forest remnant located in southeastern Brazil and (ii) to investigate possible correlations between these variables of the hydrological cycle in a forest site and seek a better understanding of the forest interference in these variables.

## Material and methods

### Study area and data collection

This study was carried out in a semideciduous seasonal forest of 6.54 ha at the coordinates of 21° 13’ 40’’ S and 44° 57’ 50’’ W, in a Dystroferric Red Latosol (Junqueira Junior et al., 2017). The Köppen-type climate is Cwb, with dry winters and rainy summers and strong seasonality of the rainfall (Junqueira Junior et al., 2017). The rainy season comprises the months from October to March and the dry season lasts from April to September. The mean annual precipitation is 1511 mm, with 85% concentrated in summer (Junqueira Junior et al., 2017).

Data collection was carried out in 2014 and 2015, and the total amount of rainfall was 1006.48 mm and 1,433.86 mm, respectively. The period of the study was characterized as an atypical drought period, since the hydrological year 2014/2015 (October-September) was one of the driest years ever observed in the region (Coelho et al., 2016).

Thirty-two measurement points were randomly distributed within the forest. Each monitoring point was monitored with a manual rain gauge, stemflow measurement apparatus (Terra et al., 2018) and a profile probe tube (PR2/6 capacitance probe from Delta-T Devices, Cambridge, UK) for soil moisture reading points up to one meter in depth. Precipitation above the canopy was obtained by a rain gauge (manual and automatic) located at the top of a 22-m high weather observation tower (Figure 1).

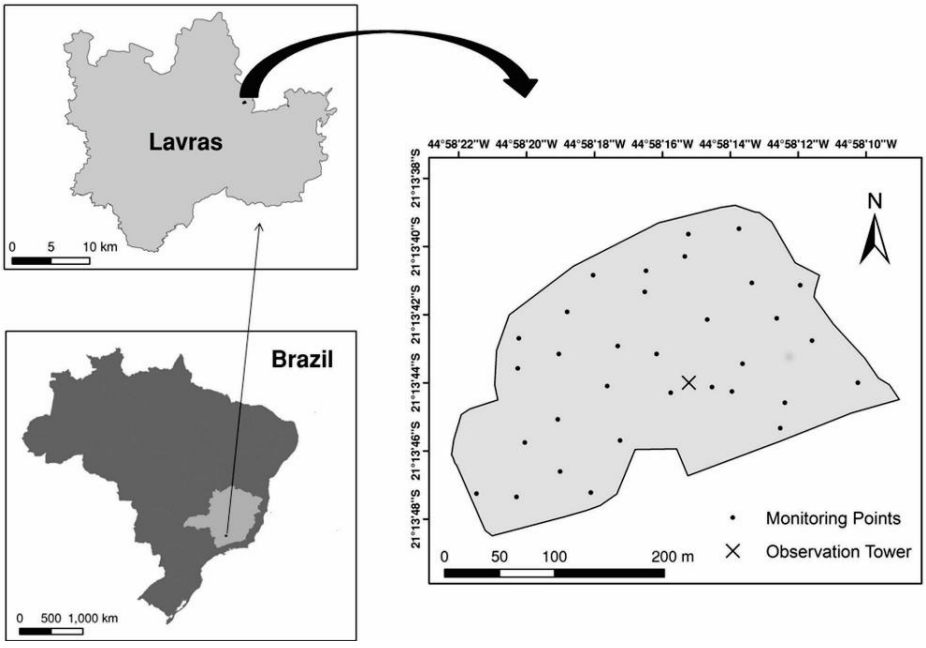


**Figure 1.** Atlantic forest remnant (study site) geographical location with the monitoring points.

Throughfall (Tf) and stemflow (Sf) collections were made on the day following each precipitation event, summed point to point and accumulated monthly, which resulted in the series of total NP (Tf + Sf). Soil moisture was also measured monthly, with the exception of April (2015) due to problems with the equipment, and integrated over the soil profile to obtain the SWC as follows Equation 1:

$$\text{SWC} = \sum_{i=1}^{n} \left( \frac{\theta_i + \theta_{i+1}}{2} \times h \right) \quad (1)$$

where:

i is the soil profile layer; n is the number of depths sampled; $\theta_i$ and $\theta_{i+1}$ are the volumetric moisture at the adjacent depths; and h is the difference in depth between the points.

### Data analysis

The SWC and NP of the two years under study were grouped and analyzed in accordance with the seasons of year-spring (October - December), summer (January - March), autumn (April - June) and winter (July - September) - since the region presents well-defined seasons and expressive differences of the variables.

The study of spatial dependence was conducted on the basis of the empirical semivariogram. For databases that presented discrepant values, a logarithmic transformation of the variable was adopted (Webster & Oliver, 2007). For an application of theoretical spatial models, anisotropy verification of the data in the directions of 0, 45, 90, and 135° was performed (Isaaks & Srivastava, 1989). The exponential model was then fitted using the weighted least squares method (Isaaks & Srivastava, 1989), since it generates a better spatial behavior description of the studied hydrological variables, especially SWC and precipitation (Mello et al., 2011; Mello, Viola, Curi, & Silva, 2012; Liang et al., 2014).

The quality of the fitted models was verified based on a cross-validation technique from which reduced mean error (RME) and reduced error standard deviation (RESD) precision statistics were calculated. The spatial dependence degree (SDD) was also calculated (Equation 2) and classified as weak (< 25%), moderate (25 ⩽ SDD ⩽ 75%) and strong (> 75%) spatial structures (adapted from Cambardella et al., 1994).

$$\text{SDD} = \frac{C_1}{C_0 + C_1} \quad (2)$$

where:

$C_1$ is the sill and $C_0$ is the nugget effect.

In addition, the spatial dependence degree was tested using the methodology proposed by Seidel and Oliveira (2014) using the so-called spatial dependence index (SDI). These authors categorically classified SDI as weak (⩽ 6%), moderate (6% < SDI ⩽ 13%) and strong (> 13%) (Seidel & Oliveira, 2016). This new proposal adds the maximum distance between the points sampled, the practical range and the respective fitted model to the SDD in order to seek a better characterization of the spatial dependence (Equation 3).

$$\text{SDI} = 0.317 \times \left( \frac{C_1}{C_0 + C_1} \right) \times \left( \frac{r}{0.5\text{MD}} \right) \times 100 \quad (3)$$

where:

r is the practical range and MD is the maximum distance between sampled points.

Subsequently, maps of the variables were compared visually and by the Pearson correlation of the data extracted from the geostatistical interpolations. The mesh is composed of 5 × 5 m pixels, totaling 4697 points. Finally, to evaluate the correlation significance, the Student's t-test was applied at 5% significance. All statistical and geostatistical analyses were performed using the R package geoR (Ribeiro Júnior & Diggle, 2001). The interpolation maps were constructed with the aid of ArcGIS 10.1 (Environmental Systems Research Institute [Esri], 2012).

## Results and discussion

### Exploratory analyses

The precipitation that reaches the canopy (gross precipitation) varied significantly throughout the year following the seasonal behavior of the climate. Spring and summer contributed 78.23% (787.4 mm) and

75.17% (1,000.7 mm) to the gross precipitation in 2014 and 2015, respectively; however, they were below the average value (85%) expected for the region under normal climate conditions. This result shows an intra-annual variability of NP that influences the SWC dynamics under a prolonged drought period, such as the 2014/2015 hydrological year.

The lack of a trend in the SWC and NP datasets could be confirmed through data exploratory analyses. Boxplot graphics showed the presence of discrepant values (outliers) in June, July and August of 2015. Such values were removed and not used in the subsequent analyses. The directional semivariograms have demonstrated an isotropic aspect for the SWC within the range from which there is spatial dependence. Ávila, Mello, and Silva (2010) studied the spatial variability of soil moisture in the layer of 0 - 0.20 m in an Atlantic rainforest and found isotropic semivariograms. Therefore, the SWC in the studied Atlantic forest fragment presented a small anisotropic characteristic, which would not affect the semivariogram modeling considering a unidirectional pattern.

The NP also presented an isotropic pattern. However, studies that attempt to characterize the spatial continuity of NP are still scarce and are concentrated in the throughfall fraction (Fang, Zhao, & Jian, 2016), since the stemflow accounts for a small amount of rain when compared to the throughfall amount (Terra et al., 2018), especially in the spring/summer seasons. Most studies that aimed to assess the throughfall spatial variability had been conducted considering only the coefficient of variation (Kowalska, Boczoń, Hildebrand, & Polkowaska, 2016); thus, the preliminary assessment of the anisotropy is a novelty and should be considered in future studies.

## Semivariogram modeling for the soil water content (SWC)

The exponential model parameters fitted to the semivariograms for SWC are shown in Table 1. A small part of the fittings presented nugget effect larger than zero, thus demonstrating the ability of the model to explain SWC spatial continuity, even at a small scale (short distances). Similarly, in the study of Ávila, Mello, Mello, and Silva (2011) for the soil moisture in the layer of 0 - 0.20 m, the exponential model did not produce a nugget effect in almost all observations. Such evidence demonstrates that the exponential model is capable of picturing the spatial variability of SWC, reducing the uncertainties. Along with the parameter analyses, cross-validation based on RME and RESD statistically proved the goodness of fit once the values of the first were close to zero and the second were close to one.

**Table 1.** Exponential model parameters fitted to SWC in the Atlantic forest remnant and their respective cross-validation statistics.

| Month | $C_0$ | $C_1$ | $a$ | RME | RESD |
|---|---|---|---|---|---|
| Jan/14 | 630.72 | 2581.79 | 76.26 | -0.004 | 1.003 |
| Feb/14 | 0.000 | 1509.68 | 43.64 | -0.014 | 1.025 |
| Mar/14 | 452.39 | 1273.25 | 84.61 | 0.002 | 0.931 |
| Apr/14 | 679.89 | 1736.64 | 83.15 | -0.005 | 0.991 |
| May/14 | 0.000 | 2648.56 | 66.04 | -0.003 | 1.120 |
| Jun/14 | 0.000 | 1761.88 | 73.42 | -0.003 | 1.096 |
| Jul/14 | 612.30 | 1962.23 | 125.46 | -0.004 | 0.978 |
| Aug/14 | 0.000 | 2273.95 | 146.84 | 0.005 | 1.116 |
| Sep/14 | 431.99 | 2057.25 | 159.71 | -0.002 | 0.925 |
| Oct/14 | 0.000 | 1529.64 | 68.64 | -0.014 | 1.075 |
| Nov/14 | 0.000 | 4800.64 | 79.80 | -0.011 | 1.088 |
| Dec/14 | 0.000 | 1822.86 | 86.46 | -0.023 | 1.132 |
| Jan/15 | 0.000 | 1855.88 | 78.60 | -0.023 | 0.987 |
| Feb/15 | 0.000 | 1635.35 | 20.24 | -0.007 | 0.930 |
| Mar/15 | 0.000 | 5362.90 | 107.88 | -0.012 | 1.138 |
| May/15 | 0.000 | 1162.03 | 25.24 | 0.001 | 0.962 |
| Jun/15* | 0.000 | 0.01 | 120.00 | -0.006 | 1.193 |
| Jul/15* | 0.000 | 0.01 | 50.00 | -0.005 | 1.087 |
| Aug/15* | 0.0024 | 0.005 | 80.00 | -0.001 | 0.996 |
| Sep/15 | 0.000 | 2546.13 | 42.15 | -0.004 | 1.001 |
| Oct/15 | 373.81 | 1310.98 | 109.50 | -0.001 | 0.998 |
| Nov/15 | 0.000 | 2398.58 | 81.47 | -0.014 | 1.067 |
| Dec/15 | 0.000 | 2560.65 | 74.77 | -0.010 | 1.034 |

*Data with logarithmic transformation.

The fitted theoretical range parameters for SWC situations showed distinct behaviors when analyzed by the seasons. In the summer and spring (wet period), the SWC had a mean theoretical range of 68.54 ± 31.37 and 83.44 ± 14.14 m, respectively. On the other hand, the ranges were 73.41 ± 34.06 m in the autumn and 100.69 ± 50.30 in the winter (dry period). These values show that the wet season exhibits smaller mean values of the spatial dependence range compared to the dry season, indicating greater variability in the former seasons. This variability is mainly due to canopy heterogeneity that leads to different spatial patterns of interception and throughfall distribution inside the forest. Nevertheless, when analyzed apart, the SWC spatial range in the autumn is lower than in the spring. This is because autumn is successive to summer and still presents high soil moisture compared to spring, which follows the dry winter of the region and requires more time for the rainfall events to proportionally increase the SWC up to a depth of 1.0 m. Therefore, for a better spatial assessment of SWC, the monitoring has to take into account different maximum distances between samples in each season because the influence of the spatial dependence varies throughout the year.

For the fitted SWC semivariogram models, the SDD was assessed and compared to the SDI (Table 2). The SDD parameter classified the spatial dependence of SWC as 'strong' in almost all the evaluated months except for March (2014), April (2014) and August (2015), for which a moderate SDD was obtained. For these months, lower spatial dependence behavior was obtained because of the random spatial variability in small distances (h), with a larger nugget effect (C0) and, consequently, a smaller sill (C1).

The abovementioned three months, which showed a moderate SDD for SWC, were classified as 'strong' by the SDI (> 13%); however, February (2015) was reclassified as having a moderate spatial structure. A plausible explanation consists of the consideration of the ratio between the practical range (r) and the half of the maximum distance between the points (169.54 m), since the situations that improved their classification have a practical range larger than this value. The same explanation may be applied for February (2015), but in the opposite way, due to the practical range being 64% lower than half of the maximum distance.

## Semivariogram modeling for net precipitation (NP)

In the case of NP (Table 3), the exponential model also produced adequate fitting (RME and RESD are close to 0 and 1, respectively). However, for April (2015) and July (2015), it was not possible to achieve a fitted semivariogram due to the low gross precipitation (3.25 and 1.5 mm, respectively). Thus, the rain was entirely intercepted and evaporated from the forest canopy.

**Table 2.** Spatial dependence degree (SDD), spatial dependence index (SDI) and practical range (*r*) of SWC with the respective classifications of the model structure.

| Month | SDD | Classification | SDI | Classification | *r* |
|---|---|---|---|---|---|
| Jan/14 | 80.37 | strong | 25.48 | strong | 228.77 |
| Feb/14 | 100.00 | strong | 24.48 | strong | 130.91 |
| Mar/14 | 73.78 | moderate | 23.39 | strong | 253.82 |
| Apr/14 | 71.87 | moderate | 22.78 | strong | 249.45 |
| May/14 | 100.00 | strong | 31.70 | strong | 198.12 |
| Jun/14 | 100.00 | strong | 31.70 | strong | 220.26 |
| Jul/14 | 76.22 | strong | 24.16 | strong | 376.38 |
| Aug/14 | 100.00 | strong | 31.70 | strong | 440.51 |
| Sep/14 | 82.65 | strong | 26.20 | strong | 479.14 |
| Oct/14 | 100.00 | strong | 31.70 | strong | 205.92 |
| Nov/14 | 100.00 | strong | 31.70 | strong | 239.40 |
| Dec/14 | 100.00 | strong | 31.70 | strong | 259.38 |
| Jan/15 | 100.00 | strong | 31.70 | strong | 235.80 |
| Feb/15 | 100.00 | strong | 11.35 | moderate | 60.71 |
| Mar/15 | 100.00 | strong | 31.70 | strong | 323.63 |
| May/15 | 100.00 | strong | 14.16 | strong | 75.72 |
| Jun/15 | 100.00 | strong | 31.70 | strong | 360.00 |
| Jul/15 | 100.00 | strong | 28.05 | strong | 150.00 |
| Aug/15 | 65.22 | moderate | 20.67 | strong | 240.00 |
| Sep/15 | 100.00 | strong | 23.64 | strong | 126.45 |
| Oct/15 | 77.81 | strong | 24.67 | strong | 328.51 |
| Nov/15 | 100.00 | strong | 31.70 | strong | 244.42 |
| Dec/15 | 100.00 | strong | 31.70 | strong | 224.32 |

The NP spatial dependence mean theoretical range parameter showed behavior similar to summer (25.81 ± 14.91 m), winter (24.32 ± 8.47 m), spring (19.90 ± 11.90 m) and autumn (41.86 ± 41.46 m). The lowest differences of the ranges among the seasons reveal that the influence of the seasonality of the rainfall is not the main factor that affects the NP spatial variability, but rather, the semideciduous behavior of the studied forest (up to 50% of the trees lose their leaves in the dry period) plays a large role.

A strong spatial dependence for NP based on the SDD for all months could be observed (Table 4). However, considering only the sill and nugget effect overestimated the spatial dependence structure in this case.

**Table 3.** Exponential model parameters fitted to NP in the Atlantic forest remnant and their respective cross-validation statistics.

| Month | $C_0$ | $C_1$ | $a$ | RME | RESD |
|---|---|---|---|---|---|
| Jan/14 | 0.000 | 767.84 | 14.62 | -0.0041 | 0.8785 |
| Feb/14 | 0.000 | 34.77 | 13.53 | -0.0004 | 0.9397 |
| Mar/14 | 0.000 | 105.88 | 9.93 | 0.0003 | 0.9179 |
| Apr/14* | 0.000 | 0.01 | 25.00 | -0.0041 | 0.9575 |
| May/14 | 0.000 | 19.82 | 115.88 | -0.0238 | 1.1196 |
| Jun/14 | 0.000 | 0.64 | 23.76 | 0.0061 | 0.8952 |
| Jul/14 | 0.000 | 68.65 | 25.34 | -0.0034 | 0.9049 |
| Aug/14 | 0.000 | 1.99 | 26.57 | -0.0066 | 0.9751 |
| Sep/14 | 0.000 | 9.77 | 21.58 | 0.0028 | 0.9726 |
| Oct/14 | 0.000 | 153.98 | 43.15 | 0.0000 | 0.8576 |
| Nov/14 | 0.000 | 699.30 | 18.01 | -0.0017 | 0.8948 |
| Dec/14 | 0.000 | 864.54 | 17.77 | -0.0015 | 0.9141 |
| Jan/15 | 0.000 | 169.43 | 33.50 | -0.0030 | 0.9841 |
| Feb/15 | 0.000 | 1621.42 | 45.07 | 0.0031 | 0.9240 |
| Mar/15 | 0.000 | 671.24 | 38.22 | -0.0143 | 1.0428 |
| May/15 | 0.000 | 187.51 | 25.69 | -0.0068 | 0.9099 |
| Jun/15 | 0.000 | 27.90 | 18.99 | -0.0009 | 0.8993 |
| Aug/15 | 0.000 | 13.23 | 12.46 | -0.0031 | 0.8704 |
| Sep/15 | 0.000 | 634.06 | 35.85 | 0.0057 | 0.9631 |
| Oct/15 | 0.000 | 8.17 | 15.83 | -0.0034 | 0.9166 |
| Nov/15 | 0.000 | 954.45 | 8.57 | -0.0007 | 0.9154 |
| Dec/15 | 0.000 | 1099.57 | 16.08 | -0.0041 | 0.9380 |

*Data with logarithmic transformation.

**Table 4.** Spatial dependence degree (SDD), spatial dependence index (SDI) and practical range ($r$) of NP with the respective classifications of the model structure.

| Month | SDD | Classification | SDI | Classification | $r$ |
|---|---|---|---|---|---|
| Jan/14 | 100.00 | strong | 8.20 | moderate | 43.85 |
| Feb/14 | 100.00 | strong | 7.59 | moderate | 40.58 |
| Mar/14 | 100.00 | strong | 5.57 | weak | 29.79 |
| Apr/14 | 100.00 | strong | 14.02 | strong | 75.00 |
| May/14 | 100.00 | strong | 31.70 | strong | 115.88 |
| Jun/14 | 100.00 | strong | 13.33 | strong | 71.29 |
| Jul/14 | 100.00 | strong | 14.21 | strong | 76.01 |
| Aug/14 | 100.00 | strong | 14.90 | strong | 79.71 |
| Sep/14 | 100.00 | strong | 12.10 | moderate | 64.73 |
| Oct/14 | 100.00 | strong | 24.20 | strong | 129.45 |
| Nov/14 | 100.00 | strong | 10.10 | moderate | 54.03 |
| Dec/14 | 100.00 | strong | 9.97 | moderate | 53.31 |
| Jan/15 | 100.00 | strong | 18.79 | strong | 100.51 |
| Feb/15 | 100.00 | strong | 25.28 | strong | 135.22 |
| Mar/15 | 100.00 | strong | 21.44 | strong | 114.67 |
| May/15 | 100.00 | strong | 14.41 | strong | 77.07 |
| Jun/15 | 100.00 | strong | 10.65 | moderate | 56.96 |
| Aug/15 | 100.00 | strong | 6.99 | moderate | 37.38 |
| Sep/15 | 100.00 | strong | 20.11 | strong | 107.55 |
| Oct/15 | 100.00 | strong | 8.88 | moderate | 47.48 |
| Nov/15 | 100.00 | strong | 4.81 | weak | 25.71 |
| Dec/15 | 100.00 | strong | 9.02 | moderate | 48.25 |

The SDI better explained the spatial dependence of this hydrological variable. Therefore, a reduction of the spatial dependence degree structure based on SDI was predominately observed because nine situations were reclassified as 'moderate' and two as 'weak'. This occurred because the practical range reached by the models is smaller than half of the maximum distances among points, showing that even though the spatial structure was well explained in the beginning of the semivariogram, the dependence relationship between the points does not reach large distances. Thus, the assessment of the spatial structure degree of the NP was more affected when considering the SPI formulation, since it accounts for more parameters that directly influence the spatial dependence. This result reinforces the need to increase the number of collectors, which should be made in shorter distances in the experimental area.

## Mapping of the SWC and NP inside the Atlantic forest remnant

Table 5 presents the SWC and NP mean values calculated by the ordinary kriging procedure. Changing SWC values demands more time than NP because the former is influenced by several intrinsic factors, such as soil physical properties and water uptake by the plant roots, i.e., the influence of the climatic seasonality throughout the years is not a unique element to be taken into consideration. This is notable when one observes the relative variation of SWC and NP during the monitoring period (SWC and NP coefficients of variation among seasons were 12.11 and 66.45%, respectively). Furthermore, the summer of 2014 was severely affected by the weather anomalous period that affected southeastern Brazil (Coelho et al., 2016), which could be detected by the geostatistical study for SWC applied here.
The maps generated by the ordinary kriging procedure are grouped in accordance with the season to compare their patterns of spatial distribution: summer (Figures 2 and 3), autumn (Figures 4 and 5), winter (Figures 6 and 7) and spring (Figures 8 and 9).

**Table 5.** Average SWC and NP for each season calculated by the ordinary kriging procedure.

| Year | Season | SWC (mm) | NP (mm) |
|---|---|---|---|
| 2014 | Summer | 287.61±23.30 | 92.84±5.50 |
| | Autumn | 268.84±23.78 | 41.24±2.98 |
| | Winter | 252.15±23.83 | 21.01±1.17 |
| | Spring | 279.11±27.73 | 134.32±6.76 |
| 2015 | Summer | 291.51±23.62 | 140.33±9.82 |
| | Autumn | 210.72±16.66 | 21.88±2.04 |
| | Winter | 217.17±17.75 | 44.66±3.69 |
| | Spring | 241.75±23.71 | 132.32±7.35 |

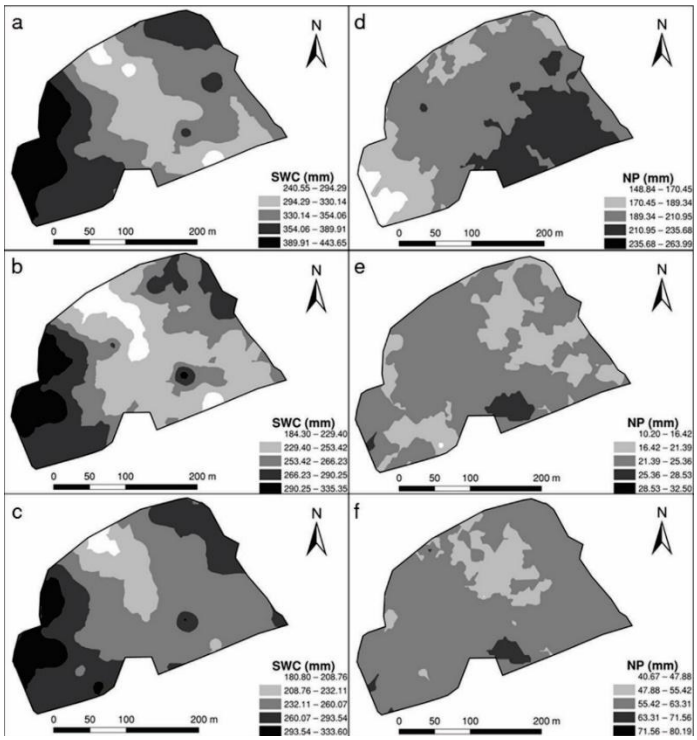


**Figure 2.** Soil water content (SWC) and net precipitation (NP) geostatistical interpolation (ordinary kriging map) for the summer of 2014. (a and d) January; (b and e) February; (c and f) March of SWC and NP, respectively, in an Atlantic forest remnant, Brazil.

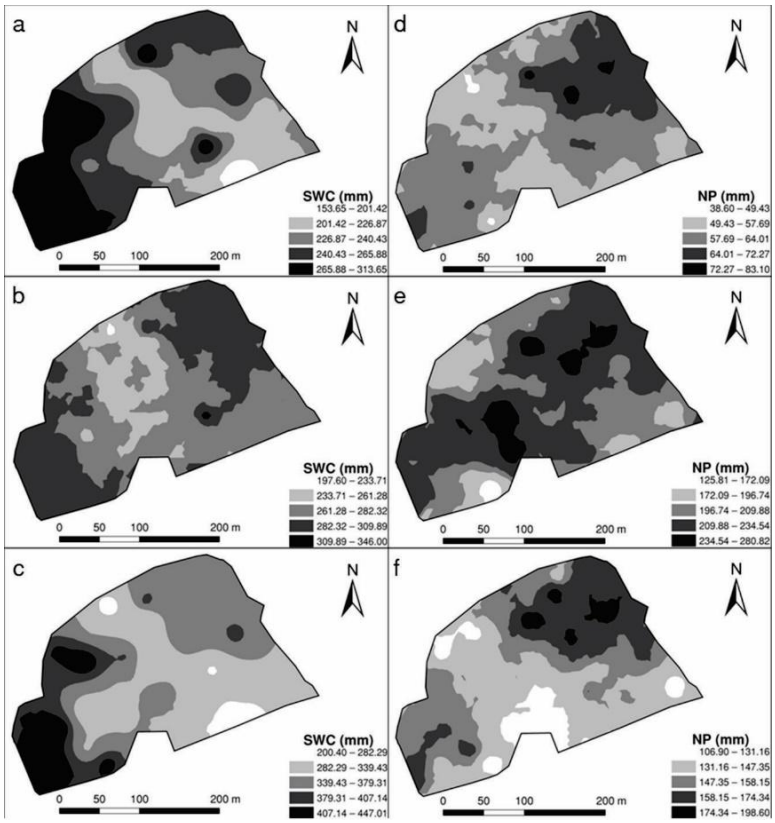


**Figure 3.** Soil water content (SWC) and net precipitation (NP) interpolation (ordinary kriging map) for the summer of 2015. (a and d) January; (b and e) February; (c and f) March of SWC and NP, respectively, in an Atlantic forest remnant, Brazil.

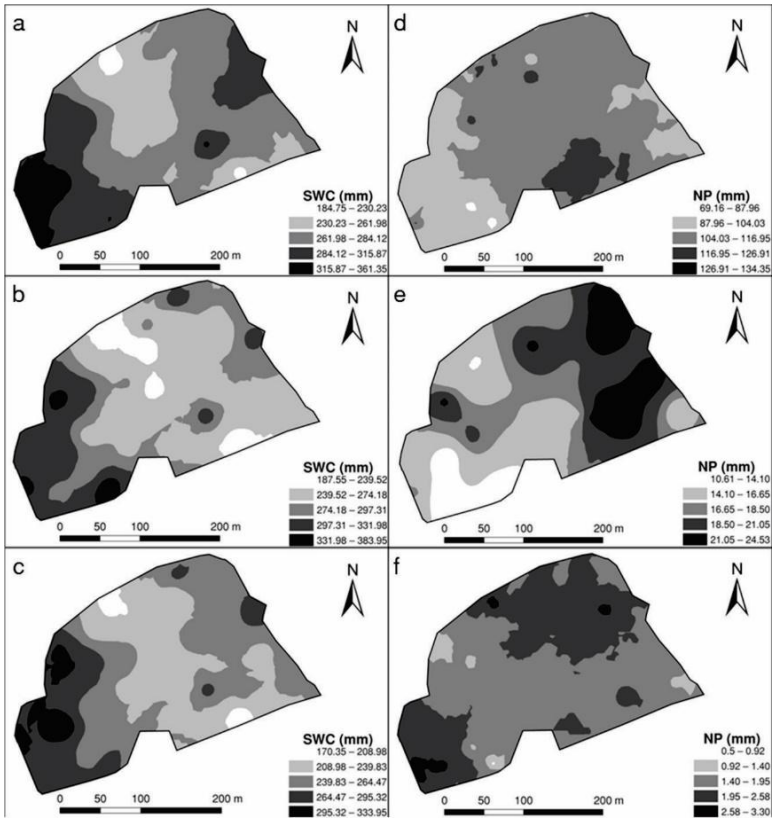


**Figure 4.** Soil water content (SWC) and net precipitation (NP) interpolation (ordinary kriging map) for autumn 2014. (a and d) April; (b and e) May; (c and f) June of SWC and NP, respectively, in an Atlantic forest remnant, Brazil.

NP maps have been demonstrated to be less smoothed for all seasons of the year due to the spatial dependence lower range and, hence, the higher variability of the maps. On the other hand, SWC showed a

more smoothed behavior throughout the year, mainly in the dry period. Such a finding may be related to the higher spatial dependence range in winter and autumn, showing small spatial variability.

Visual analyses of both variables' spatial patterns did not demonstrate a direct relationship, as NP is not the unique variable that determines the spatial behavior of SWC. The Pearson correlation coefficient between SWC and NP corroborates this, as only a few situations presented significant correlations (Jan./2014; April/2014; Aug./2014). A possible explanation is based on the fact that this study accounts for the amount of water storage in a one-meter soil profile and that there is a clear shift between soil-water redistribution and the occurrence of NP. Therefore, the correlation between NP and SWC can be significant when shallow layers are studied separately, as noted by Terra et al. (2018), who observed a positive correlation between the stemflow and the SWC in superficial layers (0 - 0.20 m) within this same study site.

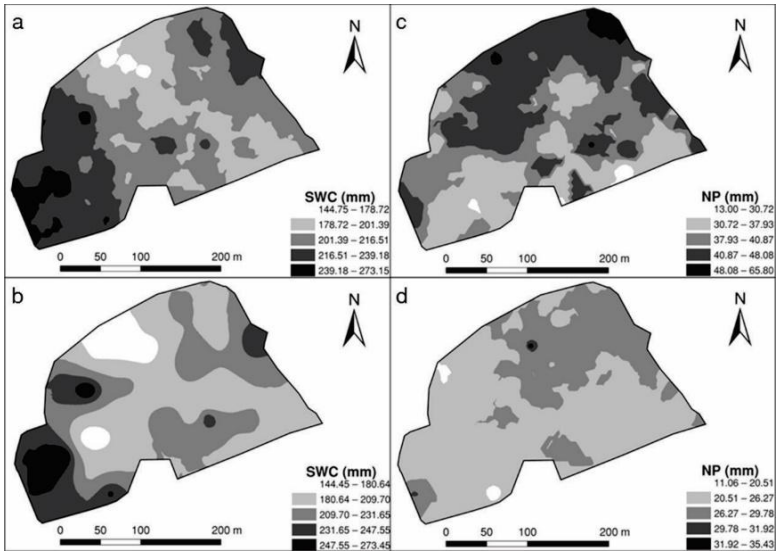


**Figure 5.** Soil water content (SWC) and net precipitation (NP) interpolation (ordinary kriging map) for autumn 2015. (a and c) May; (b and d) June of SWC and NP, respectively, in an Atlantic forest remnant, Brazil.

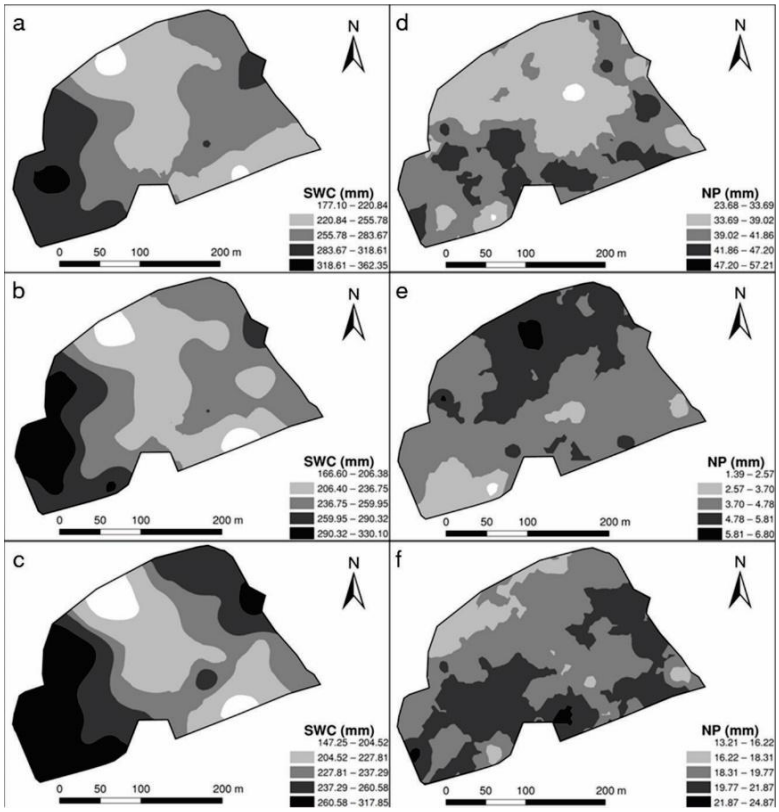


**Figure 6.** Soil water content (SWC) and net precipitation (NP) interpolation (ordinary kriging map) for winter 2014. (a and d) July; (b and e) August; (c and f) September of SWC and NP, respectively, in an Atlantic forest remnant, Brazil.

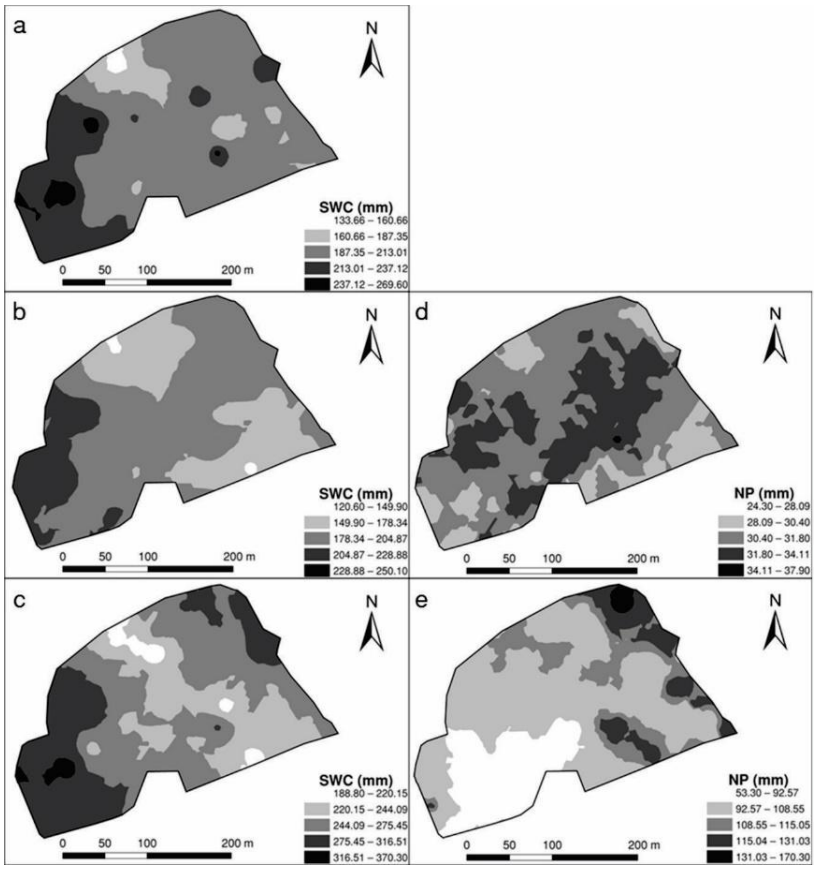


**Figure 7.** Soil water content (SWC) and net precipitation (NP) interpolation (ordinary kriging map) for winter of 2015. (a) July; (b and d) August; (c and e) September of SWC and NP, respectively, in an Atlantic forest remnant, Brazil.

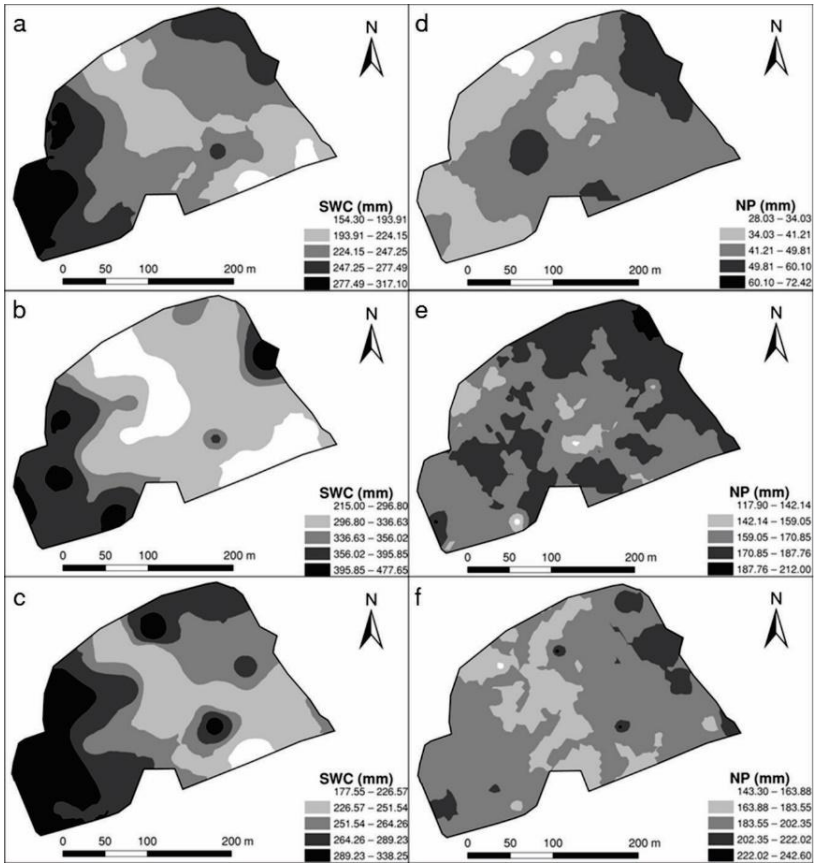


**Figure 8.** Soil water content (SWC) and net precipitation (NP) interpolation (ordinary kriging map) for spring of 2014. (a and d) October; (b and e) November; (c and f) December of SWC and NP, respectively, in an Atlantic forest remnant, Brazil.

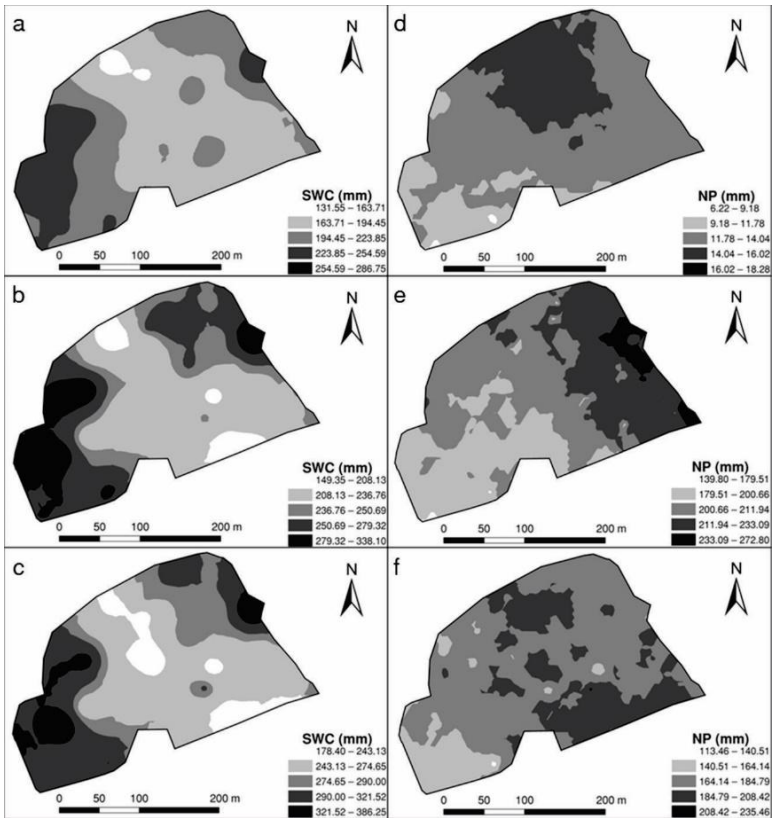


**Figure 9.** Soil water content (SWC) and net precipitation (NP) interpolation (ordinary kriging map) for spring of 2015. (a and d) October; (b and e) November; (c and f) December of SWC and NP, respectively, in an Atlantic forest remnant, Brazil.

Assessing the maps, it is remarkable that SWC, independent of the season, shows the highest values in the northeast (NE) and southwest (SW) areas and the lowest in the middle of the area. In the former areas, a smoother relief characterized the values, while the middle was more rugged. In the present study, the topography may be a key factor that influenced the results. Junqueira Junior et al. (2017) studied the temporal stability of soil moisture at different depths in this area and concluded that the temporal pattern of soil water is more related to the local topography and soil properties than canopy behavior, although these authors have not applied spatial analyses and modeling. Moreover, the visual comparative analyses between the SWC maps and the studied area slope show that the flatter areas are related to higher SWC, while the rugged areas are related to the lower values.

## Conclusion

The exponential model was able to explain the spatial behavior of both variables based on the cross-validation statistics. The SDI was shown to be important for the spatial dependence classification of NP.

The SWC has different theoretical ranges among the seasons, so that summer and autumn had smaller ranges. Therefore, when studying the spatial continuity of SWC, the sampling should consider the maximum distances for each season. For NP, similar theoretical ranges are obtained.

The NP spatial pattern was different from the SWC, with the latter being more influenced by the local topography and the former by the forest canopy.

## Acknowledgements

This work was supported by Fapemig (*Fundação de Amparo à Pesquisa do Estado de Minas Gerais*; PPM-X-045/16), CNPq (*Conselho Nacional de Desenvolvimento Científico e Tecnológico*; Processo: 401760/2016-2) and Capes (*Coordenação de Aperfeiçoamento de Pessoal de Nível Superior*; Bolsa PNPD).

## References

Ávila, L. F., Mello, C. R., & Silva, A. M. (2010). Continuidade e distribuição espacial da umidade do solo em bacia hidrográfica da Serra da Mantiqueira. *Revista Brasileira de Engenharia Agrícola e Ambiental, 14*(12), 1257-1266. DOI: 10.1590/S1415-43662010001200002

Ávila, L. F., Mello, C. R., Mello, J. M., & Silva, A. M. (2011). Padrão espaço-temporal da umidade volumétrica do solo em uma bacia hidrográfica com predominância de Latossolos. *Revista Brasileira de Ciência do Solo, 35*(5), 1801-1810. DOI: 10.1590/S0100-06832011000500034

Ávila, L. F., Mello, C. R., Pinto, L. C., & Silva, A. M. (2014). Partição da precipitação pluvial em uma microbacia hidrográfica ocupada por mata atlântica na serra da Mantiqueira, MG. *Ciência Florestal, 24* (3), 583-595. DOI: 10.1590/1980-509820142403007

Bialkowski, R., & Buttle, J. M. (2015). Stemflow and throughfall contributions to soil water recharge under trees with differing branch architectures. *Hydrological Processes, 29*(18), 4068-4082. DOI: 10.1002/hyp.10463

Cambardella, C. A., Moorman, T. B., Novak, J., Parkin, T. B., Karlen, D. L., Turco, R. F., & Konopka, A. E. (1994). Field-scale variability of soil properties in central Iowa soils. *Soil Science Society of American Journal, 58*(5), 501-1511. DOI: 10.2136/sssaj1994.03615995005800050033x

Coelho, C. A. S., Oliveira, C. P., Ambrizzi, T., Reboita, M. S., Carpenedo, C. B., Campos, J. L. P. S., ... Rehbein, A. (2016). The 2014 southeast Brazil austral summer drought: regional scale mechanisms and teleconnections. *Climate Dynamics, 46*(11-12), 3737-3752. DOI: 10.1007/s00382-015-2800-1

Environmental Systems Research Institute [Esri]. (2012). *ArcGIS 10: getting started with ArcGIS*. Retrieved on February 20, 2018 from https://www.esri.com/training/catalog/57630434851d31e02a43ef28/getting-started-with-gis/

Fang, S., Zhao, C., & Jian, S. (2016). Spatial variability of throughfall in a *Pinus tabulaeformis* plantation forest in Loess Plateau, China. *Scandinavian Journal of Forest Research, 31*(5), 467-476. DOI: 10.1080/02827581.2015.1092575

Gorenflo, L. J., Romaine, S., Mittermeier, R. A., & Walker-Painemilla, K. (2012). Co-occurrence of linguistic and biological diversity in biodiversity hotspots and high biodiversity wilderness areas. *PNAS, 109*(21), 8032-8037. DOI: 10.1073/pnas.1117511109

Isaaks, E. H., & Srivastava, R. M. (1989). *An introduction to applied geostatistics*. New York, NY: Oxford University Press.

Junqueira Junior, J. A., Mello, C. R., Owens, P. R., Mello, J. M., Curi, N., & Alves, G. J. (2017). Time-stability of soil water content (SWC) in an Atlantic Forest - Latosol site. *Geoderma, 288*, 64-78. DOI: 10.1016/j.geoderma.2016.10.034

Junqueira Junior, J. A., Mello, C. R., Mello, J. M., Scolforo, H. F., Beskow, S., & McCarter, J. (2019). Rainfall partitioning measurement and rainfall interception modelling in a tropical semi-deciduous Atlantic Forest remnant. *Agricultural and Forest Meteorology, 275*, 170-183. DOI: 10.1016/j.agrformet.2019.05.016

Kowalska, A., Boczoń, A., Hildebrand, R., & Polkowska, Z. (2016). Spatial variability of throughfall in a stand of Scots pine (Pinus sylvestris L.) with deciduous admixture as influenced by canopy cover and stem distance. *Journal of Hydrology*, *538*, 231-242. DOI: 10.1016/j.jhydrol.2016.04.023

Liang, W. L., Hung, F. X., Chan, M. C., & Lu, T. H. (2014). Spatial structure of surface soil water content in a natural forested headwater catchment with a subtropical monsoon climate. *Journal of Hydrology, 516*, 210-221. DOI: 10.1016/j.jhydrol.2014.01.032

Mello, C. R., Avila, L. F., Norton, L. D., Silva, A. M., Mello, J. M., & Beskow, S. (2011). Spatial distribution of top soil water content in an experimental catchment of Southeast Brazil. *Scientia Agricola, 68*(3), 285-294. DOI: 10.1590/S0103-90162011000300003

Mello, C. R., Viola, M. R., Curi, N., & Silva, A. M. (2012). Distribuição espacial da precipitação e da erosividade da chuva mensal e anual no estado do Espírito Santo. *Revista Brasileira de Ciencia do Solo, 36*(6), 1878-1891. DOI: 10.1590/S0100-06832012000600022

Ribeiro Júnior, P. J., & Diggle, P. J. (2001). GeoR: A package for geostatistical analysis. *R-News, 1*, 15-18.

Sari, V., Paiva, E. M. C. D., & Paiva, J. B. D. (2016). Interceptação da chuva em diferentes formações florestais na região sul do Brasil. *Revista Brasileira de Recursos Hídrico, 21*(1), 65-79. DOI: 10.21168/rbrh.v21n1.p65-79

Sato, A. M., Avelar, A. S., & Netto, A. L. C. (2011). Spatial variability and temporal stability of throughfall in a eucalyptus plantation in the hilly lowlands of southeastern Brazil. *Hydrological Processes, 25*(12), 1910-1923. DOI: 10.1002/hyp.7947

Seidel, E. J., & Oliveira, M. S. (2014). Novo índice geoestatístico para a mensuração da dependência espacial. *Revista Brasileira de Ciência do Solo, 38*(3), 699-705. DOI: 10.1590/S0100-06832014000300002

Seidel, E. J., & Oliveira, M. S. (2016). Classification for a geostatistical Index of spatial dependence. *Revista Brasileira de Ciência do Solo, 40*, 1-16. DOI: 10.1590/18069657rbcs20160007

Terra, M. C. N. S., Mello, C. R., Mello, J. M., Oliveira, V. A., Nunes, M. H., Silva, V. O., ... Alves, G. J. (2018). Stemflow in a neotropical forest remnant: vegetative determinants, spatial distribution and correlation with soil moisture. *Trees, 32*(1), 323-335. DOI: 10.1007/s00468-017-1634-3

Vale, V. S., Schiavini, I., Araújo, G. M., Gusson, A. E., Lopes, S. F., Oliveira, A. P., ... Dias-Neto, O. C. (2013). Fast changes in seasonal forest communities due to soil moisture increase after damming. *Revista de Biología Tropical, 61*(4), 1901-1917.

Webster, R., & Oliver, M. A. (2007). *Geostatistics for environmental scientists*. Chichester, GB: John Wiley & Sons Ltd.

Xu, Q., Liu, S., Wan, X., Jiang, C., Song, X., & Wang, J. (2012). Effects of rainfall on soil moisture and water movement in a subalpine dark coniferous forest in southwestern China. *Hydrological Processes, 26*(25), 3800-3809. DOI: 10.1002/hyp.8400

Yang, L., Chen, L., Wei, W., Yu, Y., & Zhang, H. (2014). Comparison of deep soil moisture in two re-vegetation watersheds in semi-arid regions. *Journal of Hydrology, 513*, 314-321. DOI: 10.1016/j.jhydrol.2014.03.049

Zucco, G., Brocca, L., Moramarco, T., & Morbidelli, R. (2014). Influence of land use on soil moisture spatial–temporal variability and monitoring. *Journal of Hydrology, 516*, 193-199. DOI: 10.1016/j.jhydrol.2014.01.043